

Electron Back Scattered Diffraction Study of Deformation and Recrystallization Textures of Constituent Phases in a Ferritic-Austenitic Duplex Steel

-Bhalchandra Vikas Bhadak-

A Dissertation Submitted to
Indian Institute of Technology Hyderabad
In Partial Fulfillment of the Requirements for
The Degree of Master of Technology



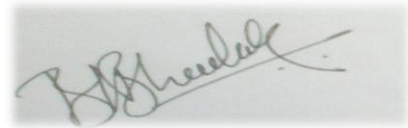
भारतीय प्रौद्योगिकी संस्थान हैदराबाद
Indian Institute of Technology Hyderabad

Department of Materials Science and Metallurgical Engineering

June, 2014

Declaration

I declare that this written submission represents my ideas in my own words, and where others' ideas or words have been included, I have adequately cited and referenced the original sources. I also declare that I have adhered to all principles of academic honesty and integrity and have not misrepresented or fabricated or falsified any idea/data/fact/source in my submission. I understand that any violation of the above will be a cause for disciplinary action by the Institute and can also evoke penal action from the sources that have thus not been properly cited, or from whom proper permission has not been taken when needed.



(Signature)

Bhalchandra Vikas Bhadak

(-Name-)

MS12M1001

(-Roll No-)


Approval Sheet

This thesis entitled “**Electron Back Scatter Diffraction Study of Deformation and Recrystallization textures of Constituent Phases in a Ferritic-Austenitic Duplex Steel**” by Bhalchandra Vikas Bhadak is approved for the degree of Master of Technology from IIT Hyderabad.



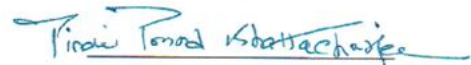
Dr. Saswata Bhattacharya

Department of Materials Science and Metallurgical Engineering
(Examiner)



Dr. B. Panigrahi

Department of Materials Science and Metallurgical Engineering
(Examiner)



-Dr. Pinaki Prasad Bhattacharjee

Department of Materials Science and Metallurgical Engineering
(Adviser)



Dr. B. Munwar Basha

Department of Civil Engineering
(Chairman)

Acknowledgements

First of all, I would like to express my deep sense of gratitude to my project guide **Dr. Pinaki Prasad Bhattacharjee**, for his esteemed guidance. He has been a role model for me and influences me in almost every aspect. His guidance and motivation helped me a lot during my post-graduate study.

I would like to thank Mr. Md. Zaid Ahemad, Mr. Dan Sathiaraj, Mr. Jagga Rao Gatti, PhD scholars for their kind attention and sharing knowledge to carry out experiments on SEM-EBSD.

I would also like to thank all my friends; Tushar, Ankit, Nida, Rahul, Manish, Vasundhara, Satyanarayana, Usha, Sushmita, Kumar and Basanth for their kind support and encouragement extended throughout the project work. We had a great time together.

Last but not the least; I would like to express my sincere thanks to all others who have directly or indirectly helped me in my project work.

Abstract

The effect of warm rolling on the evolution of microstructure, microtexture and mechanical properties of a 0.05%C-22%Cr-5%Ni duplex stainless steel (DSS) was investigated. For this purpose, the DSS alloy was homogenized at 1150°C warm rolled at 625°C up to 90% reduction of thickness. Development of ultrafine lamellar morphology with alternate arrangement of the two phases was revealed during warm rolling. The ferrite in DSS developed stronger RD-fiber (RD//<110>) than ND-fiber (ND//<111>) while austenite in DSS showed pure metal or copper type texture. Subsequently, isothermal annealing was carried out at the homogenization temperature. Gradual transformation from lamellar bamboo type morphology to more globular morphology was observed during isothermal annealing. The texture development of the two phases is not significantly affected by the presence of the other phase while the grain growth during recrystallization is strongly affected by the presence of the other phase. Ferrite in annealed DSS showed much stronger RD-fiber which indicated pronounced recovery. Austenite in DSS retained pure metal type texture i.e. recrystallization texture with no preferential orientation selection. The DSS in the as warm-rolled and annealed condition showed remarkable increase in the ultimate tensile strength to ~1.2GPa. Strength and ductility of DSS after annealing were significantly affected by different structural and morphological changes. The present results demonstrated that warm rolling could be used successfully as a novel thermo-mechanical processing route for developing ultrahigh strength DSS.

Nomenclature

DSS- Duplex Stainless Steel

WR- Warm Rolling

RD- Rolling Direction

ND- Normal Direction

TD- Transverse Direction

EBSD- Electron Back-scattered Diffraction

HAGB- High Angle Grain Boundaries

LAGB- Low Angle Grain Boundaries

BCC- Body Centered Cubic

FCC- Face Centered Cubic

SFE- Stacking Fault Energy

ODF- Orientation Distribution Function

PF- Pole Figure

Contents

Declaration	ii
Approval Sheet	iii
Acknowledgements	iv
Abstract.....	v
Nomenclature	vi
1 Introduction	1
1.1 Overview.....	1
1.2 Objective and Scope.....	1
2 Literature Review	3
2.1 Deformation and Recrystallization Behavior of Duplex Alloys.....	3
2.2 Novelty of Present Work.....	4
3 Experimental Methods	5
3.1 Thermo-mechanical Processing.....	5
3.2 Characterization.....	6
3.3 Mechanical Testing.....	7
4 Results	9
4.1 Starting Material	9
4.2 Evolution of Microstructure during Warm Rolling.....	11
4.3 Evolution of Texture during Warm Rolling.....	13
4.4 Evolution of Microstructure during Annealing.....	17
4.5 Evolution of Texture During Annealing.....	20
4.6 Mechanical Properties of DSS.....	22
5 Discussion	26
5.1 Evolution of Microstructure during Warm Rolling.....	26
5.2 Evolution of Texture during Warm Rolling.....	26
5.3 Evolution of Microstructure during Annealing.....	28
5.4 Evolution of Annealing Texture	30
5.1 Mechanical Properties of DSS.....	31
5 Summary and Conclusion	33
References	35

Chapter 1: Introduction

1.1 Overview

Plastic deformation of polycrystalline materials such as in rolling (Fig. 1) is always accompanied by development of crystallographic texture which in turn affects microstructure, texture and properties during subsequent processing. As a result the evolution of microstructure and texture has been intensely investigated in a wide variety of materials including single crystals [1] as well as polycrystalline materials [2]. However, deformation behavior of duplex alloys, such as, duplex stainless steels (DSS) where the constituent phases have different crystal structures but retain grain structure, has been studied to a much lesser extent, particularly, at the very high strain regime.

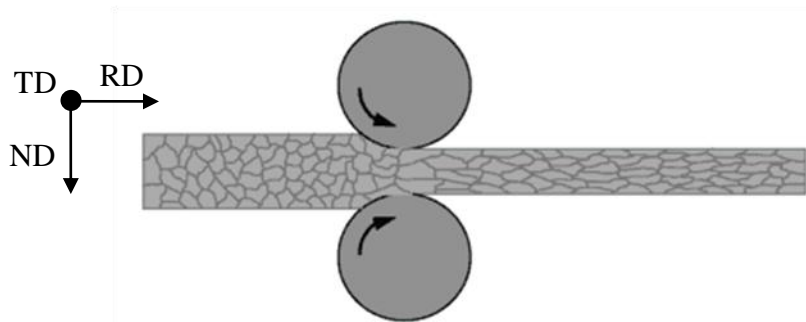


Fig. 1: Schematic of rolling process

1.2 Objective and Scope

The present work aims to improve fundamental understanding of deformation and recrystallization behavior of duplex alloys using a commercial grade duplex stainless steel (DSS) (SAF 2507; Sandvik, Sweden) having austenite (FCC) and Ferrite (BCC) as constituent phases as a model system. In order to avoid strain induced phase the deformation is carried out in the warm-working range. Interestingly, although warm-rolling has been carried out in single phase ferrite, in

DSS such studies have received little attention which constitutes a prime novelty of the present work. The effect of processing parameters, namely, strain and annealing time has been investigated in the present study. It is believed that the present study will be helpful in understanding the deformation and recrystallization behavior of other duplex grade alloys.

Chapter 2: Literature Review

2.1 Deformation and recrystallization behavior of duplex alloys

Microstructural and texture evolution during deformation and subsequent annealing of single phase materials e.g. BCC and FCC metals and alloys [3-8] and two phase alloys with second phase in the dispersed form (e.g. precipitates) [9] have been intensely investigated. However, the evolution of microstructure and texture of duplex alloys i.e. alloys having two phase structure where both the phases have grain structure for e.g. duplex stainless steels (DSS) have been studied to a much lesser extent.

DSS are composed of austenite and ferrite with equal or nearly equal fraction of the two phases, although, commercial grade alloys might also have 40% or 30% of austenite. This unique feature of DSS provides high mechanical strength, excellent resistance to stress corrosion cracking even in chloride bearing atmosphere with good weldability [10]. As a result these alloys are widely used in corrosive environments such as in chemical plants due to their excellent corrosion resistance and higher strength. However, DSS may also undergo unwanted phase transformation that can lead to reduction in toughness and decrease in corrosion resistance. Thus, for appropriate heat treatment, deformation processes and welding, a thorough knowledge of relation between microstructural evolution and different processing parameters is required DSS.

At the same time to increase the usage of DSS in structural applications proper understanding of the deformation and recrystallization behavior is required. It

is noticed that the development of microstructure and texture during deformation and recrystallization of DSS has been studied to a much lesser extent as compared to single-phase austenitic or ferritic steels in terms of effect of deformation temperature, effect of strain path change and its mechanical properties. Even then majority of the available studies are focused on the microstructure and texture evolution during cold deformation and subsequent annealing [11-16]. It has been reported that ferrite and austenite in DSS deform independent of each other leading to a deformation texture similar to the respective single-phase materials [12]. Some previous investigations have concluded that, characteristic banded structure with alternate arrangement of ferrite and austenite phases can influence texture development during cold rolling at higher reductions [17-19]. This is also influenced by prior thermo-mechanical treatment of DSS material, which can significantly affect further microstructural and texture development during subsequent annealing [20-22].

2.2 Novelty of the present work

The present research is focused on understanding the evolution of microstructure and microtexture during warm rolling and subsequent annealing of commercial grade DSS (Grade: SAF 2507, Sandvik, Sweden). Effects of warm rolling on deformation and annealing behavior of single phase material have been studied well [23-25]. The warm-rolling behavior of a custom made DSS has only been reported recently by Bhattacharjee et al [34] who have shown significant effect of warm-rolling temperature on microstructure and texture development. However, the warm-rolling behavior of commercial grade DSS (SAF 2507, Sandvik, Sweden) is yet to be revealed which constitutes the main objective of the present study.

Chapter 3: Experimental Methods

3.1 Thermo-mechanical Processing

The chemical composition of the commercial grade DSS (SAF 2507) involved in this study is summarized in Table 1.

Table 1: Chemical composition of DSS:

Element	C	S	Cr	Mn	Ni	P	Si	Mo	Fe
(Wt. %)	0.05	0.001	22.1	2.03	5.48	0.009	0.45	3.05	Balance

This material is then cut into rectangular specimens of size $20\text{mm}(\text{width}) \times 40\text{mm}$ and subjected to homogenization heat treatment in horizontal tubular furnace at 1150°C for 2hrs in an inert atmosphere (argon). The homogenized DSS specimens were soaked in a muffle furnace for 15minutes at 625°C before every warm-rolling pass and subsequently warm-rolled up to 90% reduction in thickness. This was achieved in steps of 20%, 40%, 60%, 70%, 80% to 90% using a laboratory scale rolling machine (SPX Precision Equipment, USA) having roll diameter of 140mm. The rolls were pre-heated to 250°C in order to prevent sudden quenching effect during warm rolling as shown in Fig. 2. After every warm rolling pass, samples were immediately water quenched.



Fig. 2: Rolling machine and muffle furnace setup

3.2 Characterization

The microstructure and microtexture of the deformed materials were characterized using electron back scatter diffraction system (EBSD, Oxford Instruments, UK) attached to a FEGSEM (Make: Carl Zeiss, Germany, Model: SUPRA-40). Samples for EBSD were prepared by mechanical polishing using emery papers having grit size of 1000, 1200, 1500 in that sequence. This was followed by cloth polishing using 10 μ m, 6 μ m, 3 μ m, 1 μ m abrasive pastes in that sequence. Subsequently electro-polishing using a solution consisting of 700ml ethanol, 120ml distilled water, 100ml glycerol, and 80ml perchloric acid at room temperature at potential of 27V. EBSD scans were taken in the longitudinal section (RD-ND plane). EBSD scans were acquired from the mid-thickness region (Fig. 3) to cover at least~2500 grains for statistical reliability of texture results. EBSD scans were acquired using a very fine scan step size of 5 nm maintaining similar conditions for deformed samples. The acquired EBSD dataset were analyzed using TSL-OIMTM software. For calculating the volume fraction of different texture components a cut-off angle of 15° used.

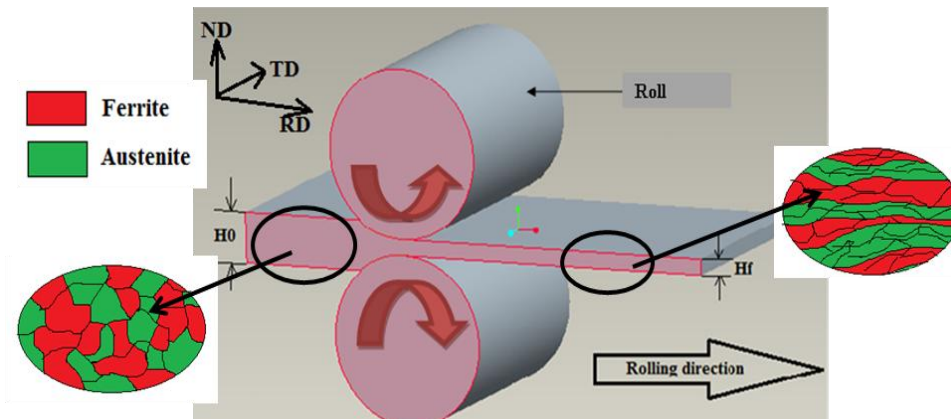


Fig. 3: Schematic of rolling of sheet with microstructure before and after rolling

3.3 Mechanical Testing

Tensile specimens were prepared along the RD from as warm rolled and annealed DSS materials. As shown in Fig. 4 all the tensile specimens were prepared having gauge length of 11mm and gauge width of 1.5mm as per the specifications of Iron and Steel Institute of Japan (ISIJ). Tensile testing was carried out using a universal testing machine (Model: 5967 Instron, 30kN load cell, UK) using a constant strain rate of 10^{-3} sec^{-1} and the loading direction was kept along the RD. Samples after tensile fracture were cut in such a way that EBSD could be carried out at the vicinity of the necked region.

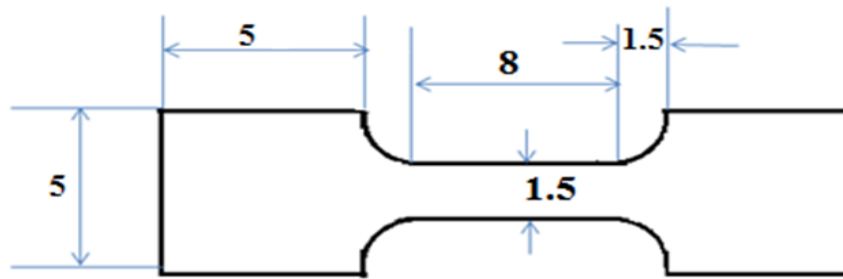


Fig. 4: Schematic of dimensions of tensile specimen. All dimensions are shown in mm.

Chapter 4: Results

4.1 Starting Material

Fig. 4.1 shows the phase map obtained from the ND-RD plane of the starting homogenized material. The ferrite is shown in red and austenite in green color. This convention for color code is followed throughout this chapter. The phase map shows elongated morphology of the two phases along the prior hot rolling direction. The volume fraction of ferrite (~60%) is slightly more than that of the austenite in the homogenized starting material. The average grain size measured along the normal direction (ND) in the RD-ND plane is very similar (~9.5 μm) for the two phases.

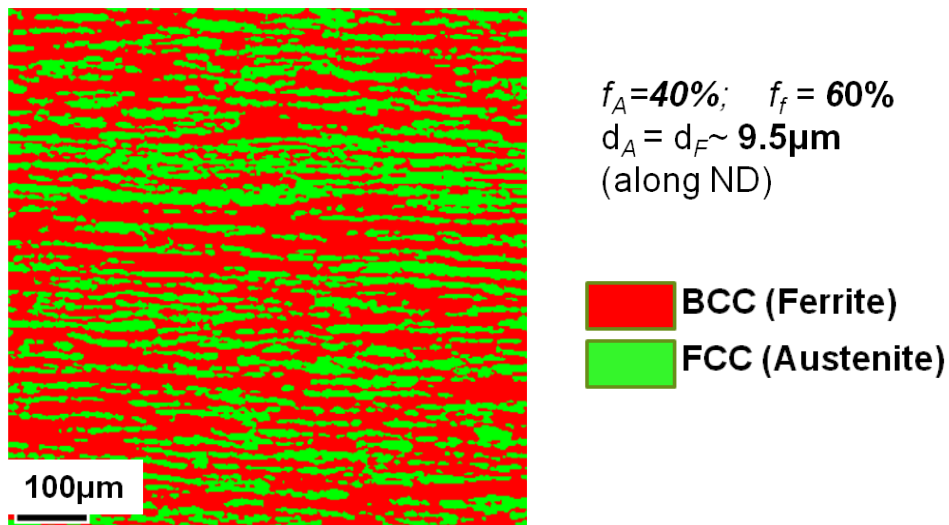


Fig. 4.1: Phase map of the starting homogenized material

The starting texture of two phases in the homogenized DSS is summarized in Fig. 4.2. Fig. 4.2(a) shows the $\varphi_2=45^\circ$ section of ODF of ferrite in DSS while Fig. 4.2(b) shows the $\varphi_2=45^\circ$ section of ODF with ideal orientations. High intensities of contour lines are found at the locations of RD-fiber components i.e. (001) $\langle 110 \rangle$, (112) $\langle 110 \rangle$; while negligible presence of

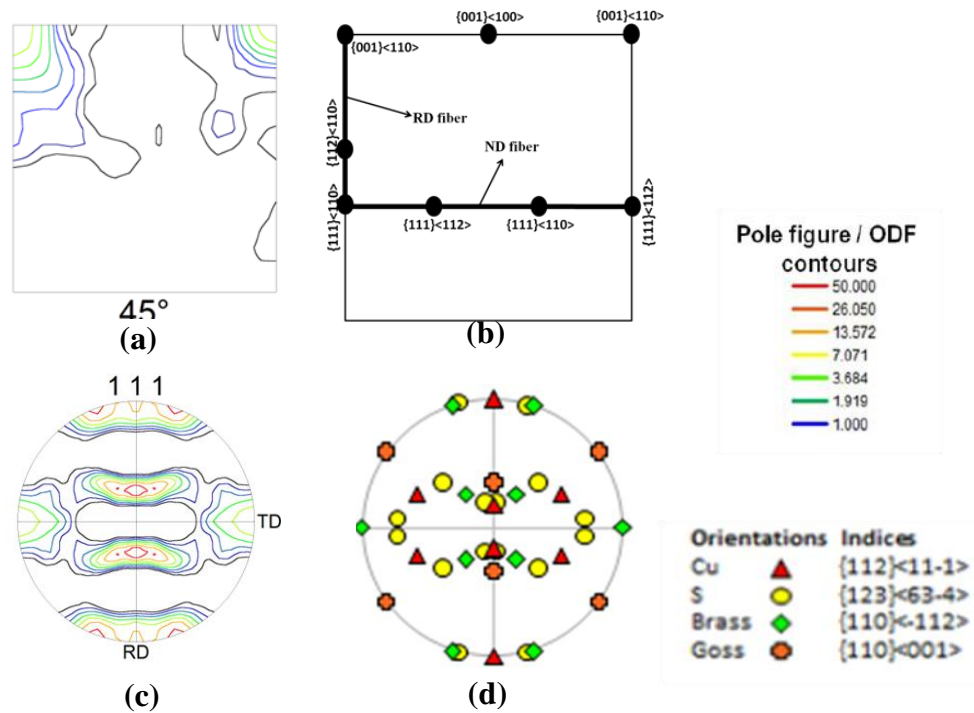


Fig. 4.2: (a) $\phi_2=45^\circ$ section of the ODF of ferrite (b) ideal $\phi_2=45^\circ$ section of ODF; (c) (111) pole figure of austenite and (d) ideal (111) pole figure of austenite

ND-fiber components are observed.

Austenite texture in DSS is shown by (111) pole figure in Fig.4.2(c) while Fig. 4.2(d) depicts the (111) pole figure with ideal locations of the texture components. The intensities of the contour lines indicates the presence of texture components Copper (or Cu): $\{(112) \langle 111 \rangle\}$, S: $\{(123) \langle 634 \rangle\}$ and brass (or Bs: $\{110\} \langle 112 \rangle\}$ with compared to the ideal positions of mentioned texture components (Fig. 4.2 (d)).

The texture of the two phases in the starting homogenized material is shown quantitatively in Fig. 4.3. Fig. 4.3(a) reveals that RD-fiber components (volume fraction ~33%) are much higher than the ND-fiber components (~8%) in ferrite of homogenized DSS. Austenite texture of DSS reveals that S is the strongest component having volume fraction ~19% followed by the Bs (~15%) and Cu (~9%) components. The quantitative analysis also amply corroborate the presence of a pure

metal type (or copper type) texture in austenite of homogenized DSS. However, the volume fraction of random components remains rather high ~55%.

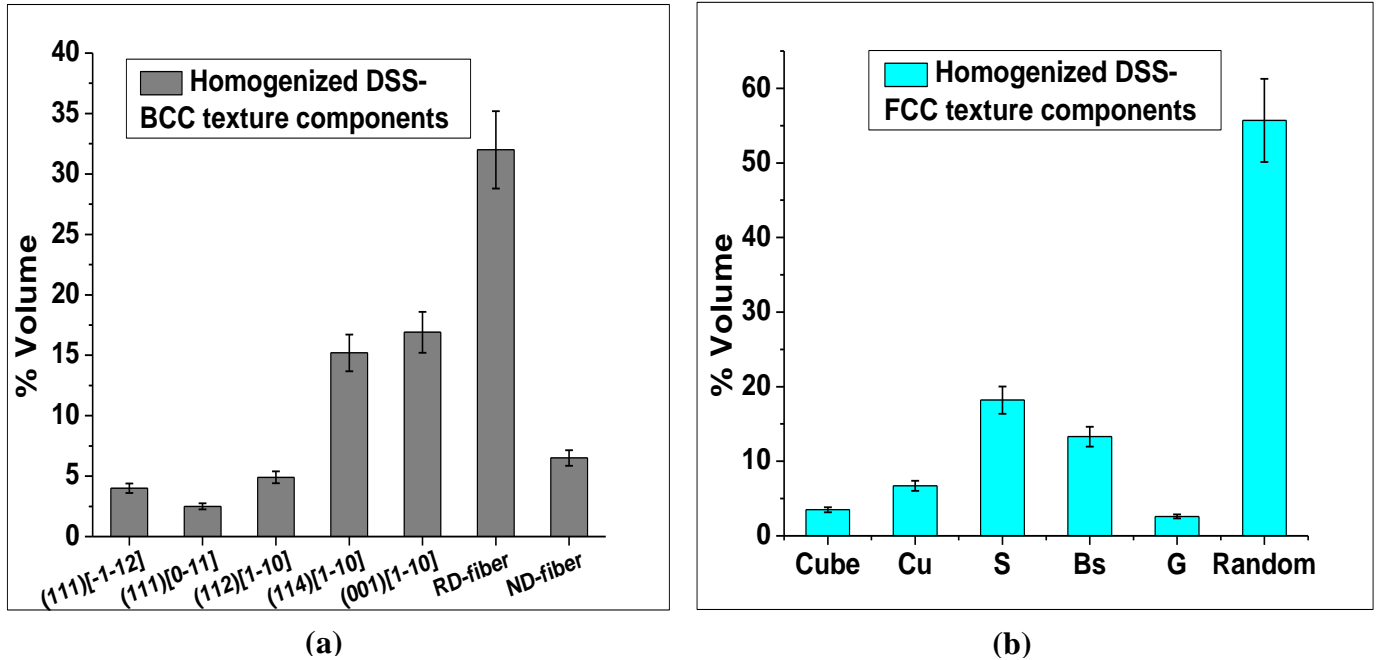


Fig. 4.3: Variation of texture components in (a) ferrite and (b) austenite in homogenized DSS

4.2 Evolution of Microstructure during Warm- Rolling

During warm rolling, microstructure gradually changes with imposed strain. This is observed in the phase maps of deformed materials at various strain levels shown in Fig. 4.4. With increasing percentage reduction the microstructure transforms into a lamellar deformation structure with alternate arrangement of the two phase bands. Further at higher reductions individual phase bands are subdivided by high angle boundaries (HABs) extended parallel to the rolling direction.

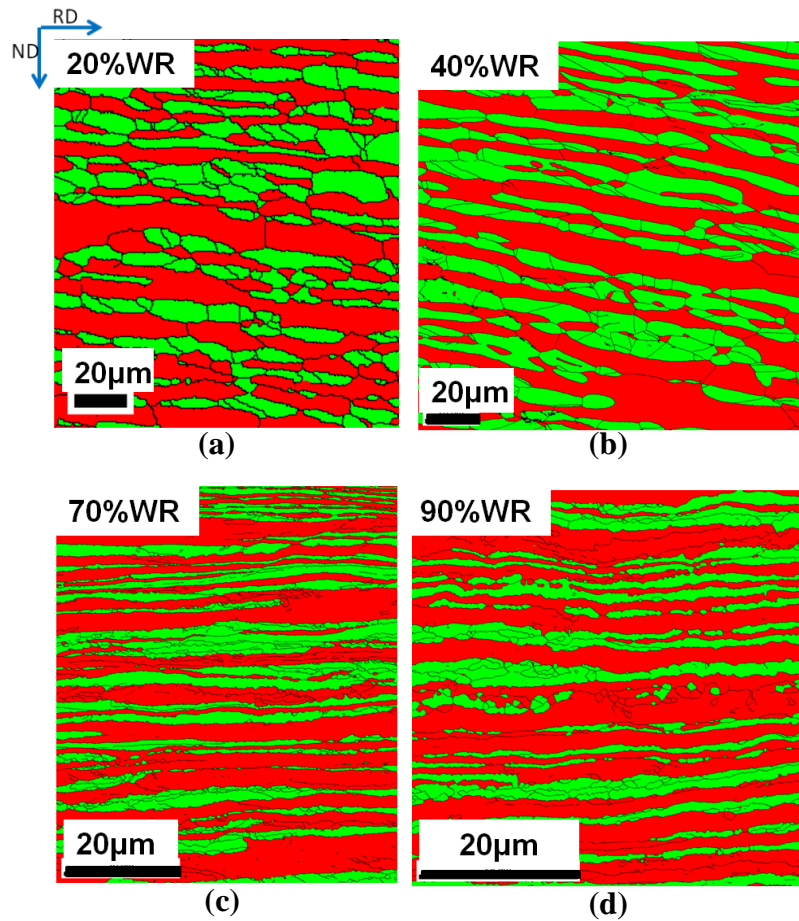


Fig. 4.4: Phase maps of warm rolled DSS at different reduction levels

Evolution of key microstructural parameters, such as, phase band thickness and grain intercept i.e. HAGB intercept along ND during warm-rolling is shown in Fig. 4.5. With increasing reduction both phase band and grain thickness are reduced. Decrease in GI is more than that of PB. The variation in HAGB fraction is shown in Fig. 4.5(b). It clearly shows that initially the fraction of HAGBs is decreased as the LAGB network is developed but the HAGB fraction increases again at higher strain level.

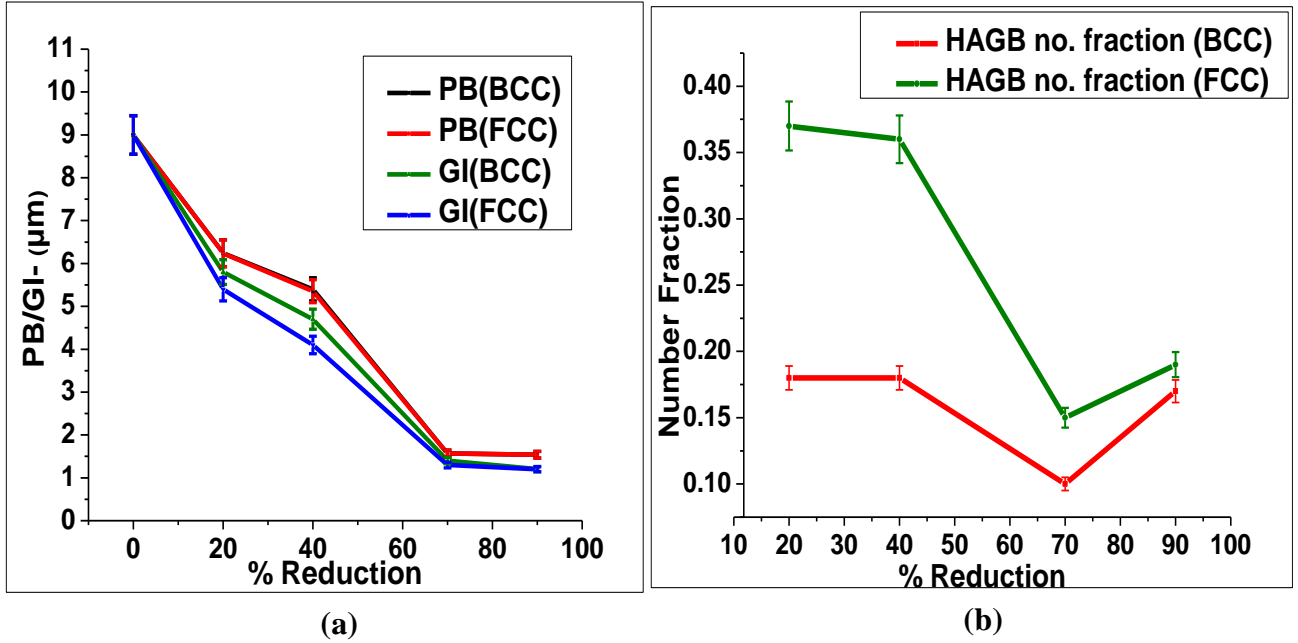


Fig. 4.5: Variation of (a) phase band and grain thickness and (b) HAGB fraction with thickness reduction

4.3 Evolution of Texture during Warm Rolling

Fig. 4.6 shows the development of texture in DSS during warm-rolling. Fig. 4.6((a)-(d)) shows the crystal orientation maps revealing the spatial distribution of different texture components of ferrite in DSS after 20% (Fig. 4.6(a)), 40% (Fig. 4.6(b)), 60% (Fig. 4.6(c)) and 90% (Fig. 4.6(d)) thickness reduction. Fig. 4.6((e)-(h)) show the $\varphi_2 = 45^\circ$ section of the ODF which clearly shows the presence of the two texture fibers, namely, RD and ND-fibers. Initially, in the 20% warm-rolled material RD-fiber is stronger than the ND-fiber (Fig. 4.6(a)) which is also evidenced in the ODF (Fig. 4.6(e)). ND-fiber is strengthened with further rolling reduction, however, RD-fiber dominates the deformation texture as may be clearly seen from the orientation maps (Fig. 4.6((b)-(d)) and the ODF (Fig. 4.6(f)-(h)). The variation in the volume fraction of two texture fibers is summarized quantitatively in Fig. 4.7.

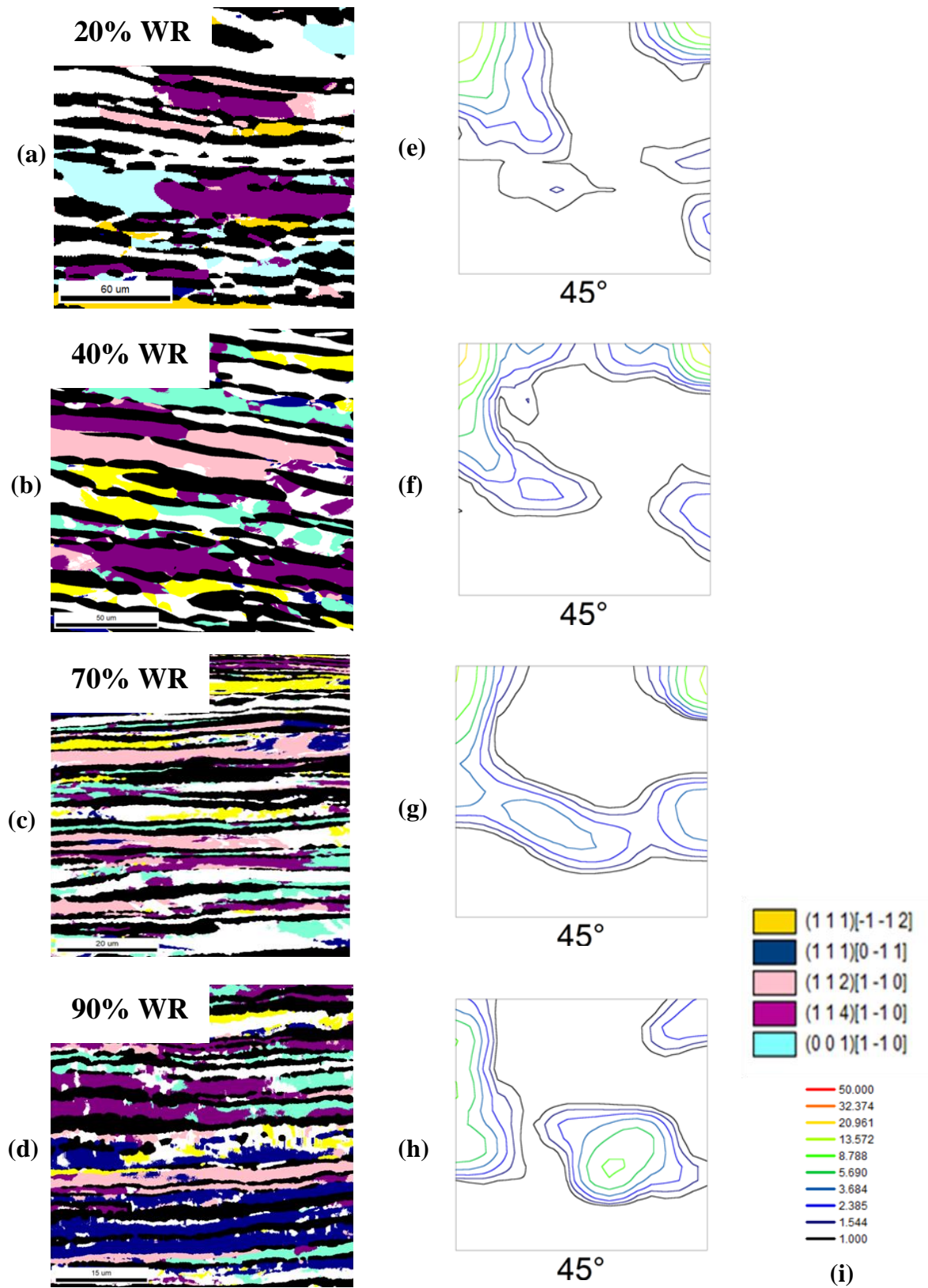


Fig. 4.6: (a)-(d) Crystal orientation maps and (e)-(h) $\phi_2=45^\circ$ section of ODF of ferrite in warm rolled DSS after 20% ((a),(e)), 40% ((b),(f)), 60% ((c),(g)) and 90% ((d),(h)) reduction in thickness.

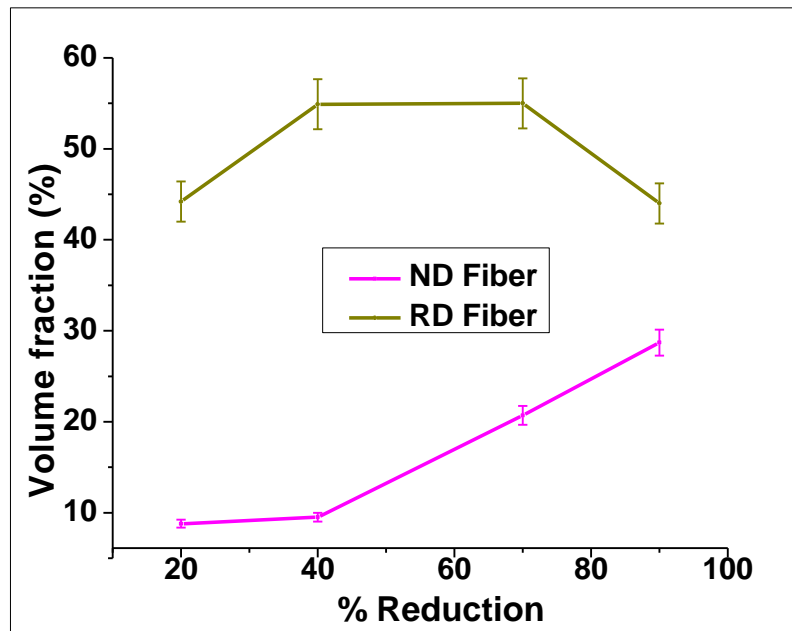


Fig. 4.7: Evolution of the two texture fibers during warm-rolling.

Fig. 4.8(a)-(d) illustrate the spatial orientation of different texture components of austenite in warm rolled DSS where the ferrite phase is masked. Initially, at lower deformations i.e. 20% and 40% warm rolled orientation maps show rather high volume fraction of random components. However, with increasing thickness reduction fraction of random components is decreased and the major components are the S (yellow), B_S (green) and the Cu (red) components. Accordingly, the (111) pole figures of austenite (Fig. 4.7 (e)-(h)) show the development of pure metal type texture. The evolution of texture components in austenite is shown quantitatively in Fig. 4.9.

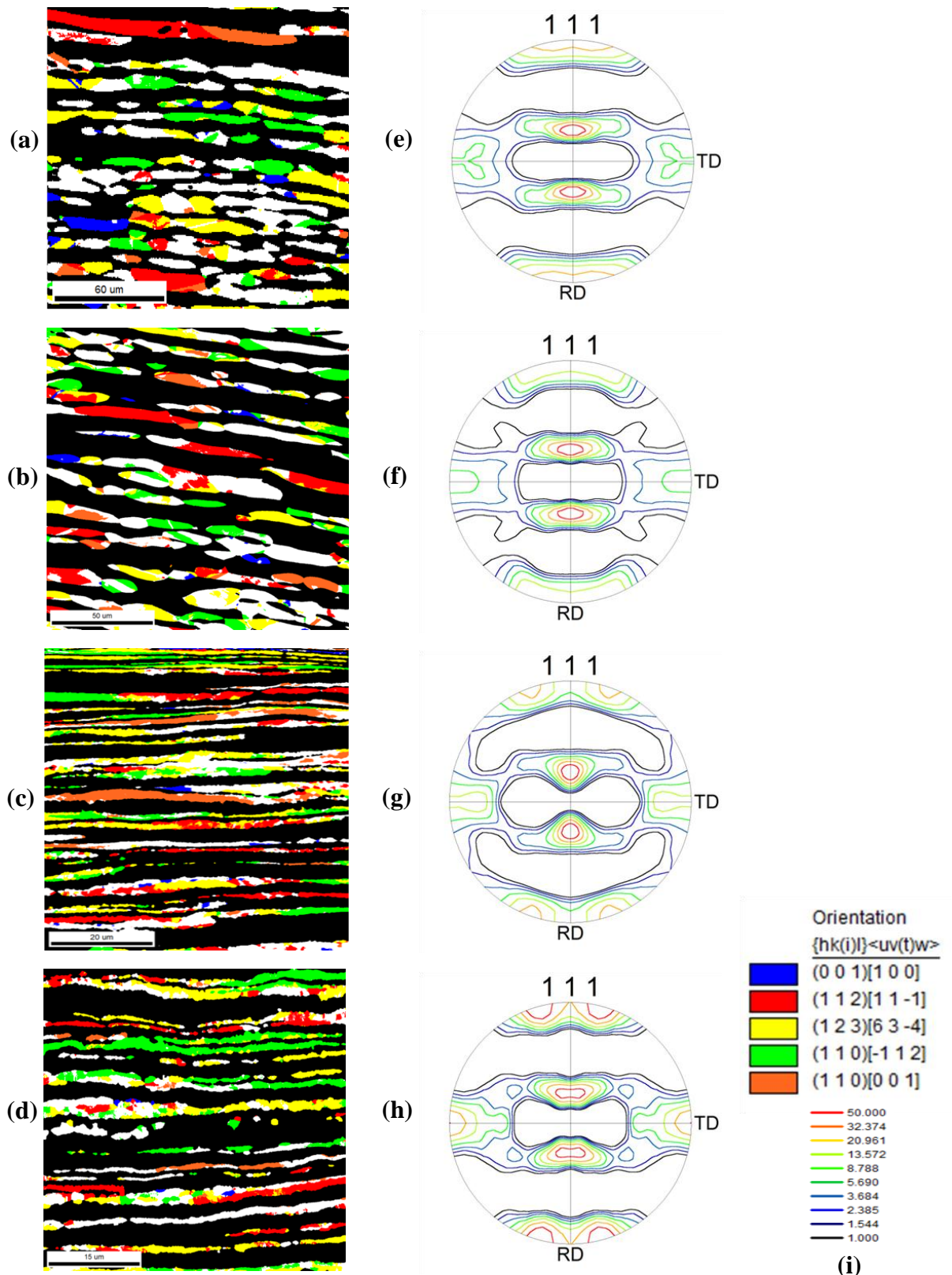


Fig. 4.8: (a)-(d) Crystal orientation maps and (e)-(h) $\phi_2 = 45^\circ$ section of ODF of austenite in warm rolled DSS after 20% ((a),(e)), 40% ((b),(f)), 60% ((c),(g)) and 90% ((d),(h)) reduction in thickness.

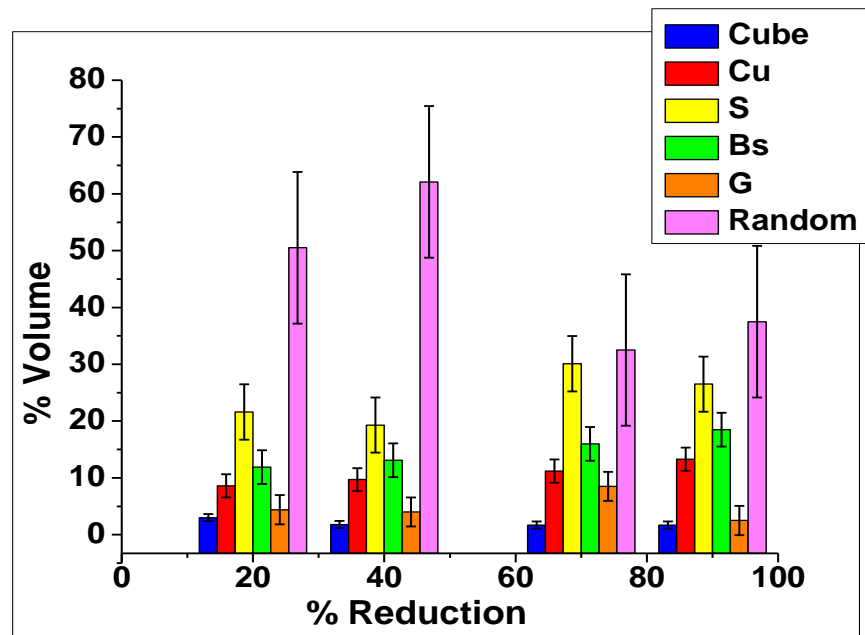


Fig. 4.9: Evolution of different texture components in austenite during warm-rolling of DSS

4.4 Evolution of Microstructure during Annealing

Microstructural evolution during isothermal annealing of warm-rolled DSS is shown in Fig. 4.10. The elongated banded morphology of the as warm-rolled material is retained after annealing for two minutes (Fig. 4.10(a)). In both the phases grain boundaries are found running perpendicular to the phase boundaries. However, in case of ferrite LAGBs (highlighted in grey) perpendicular to the phase boundaries could be observed. In contrast, in case of austenite mostly HAGBs are found normal to phase boundaries. Austenite also profuse annealing twins evidenced by the presence of annealing twin boundaries (highlighted in yellow). With increasing isothermal holding time the banded morphology of the warm-rolled structure is broken down and grains with more globular morphology is observed. This is observed more clearly in case of the specimen annealed for 60minutes (Fig. 4.10(c))

as compared to sample annealed for 30minutes (Fig. 4.10(c)). Regions showing clear break down of the lamellar structure are marked in Fig. 4.10(b) and 4.10(c).

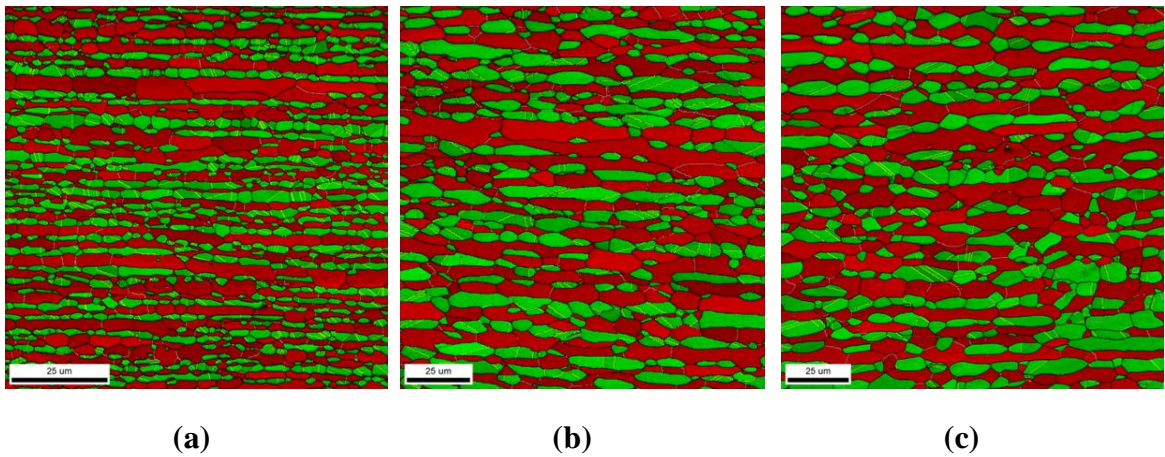


Fig. 4.10: Phase maps of annealed DSS at 1150°C at different time intervals (a) 2min (b) 30min (c) 60min

The variation in HAGB fraction in ferrite during isothermal annealing is shown in Fig. 4.11(a). HAGB fraction in ferrite in warm-rolled condition is ~15% but is found to increase during isothermal annealing for two and 30minutes. HAGB fraction is slightly decreased following annealing for 60minutes which appears to be due to grain coarsening as may be seen from the phase map (Fig. 4.10(c)).

Fig. 4.11(b) shows the variation of HAGB fraction in austenite during isothermal annealing. The HAGB fraction in austenite in as warm-rolled condition is ~54%. The HAGB fraction is increased to ~80% after annealing for two minutes but significant change is not observed during further isothermal holding. Drastic increase in annealing twin boundaries fraction ($60^\circ\langle 111 \rangle$) could be observed during isothermal annealing for two minutes. This is consistent with the presence of profuse

annealing twin boundaries (highlighted by yellow lines) observed in austenite in the phase maps of annealed materials (Fig. 4.10). The twin boundary fraction does not change significantly during further isothermal holding.

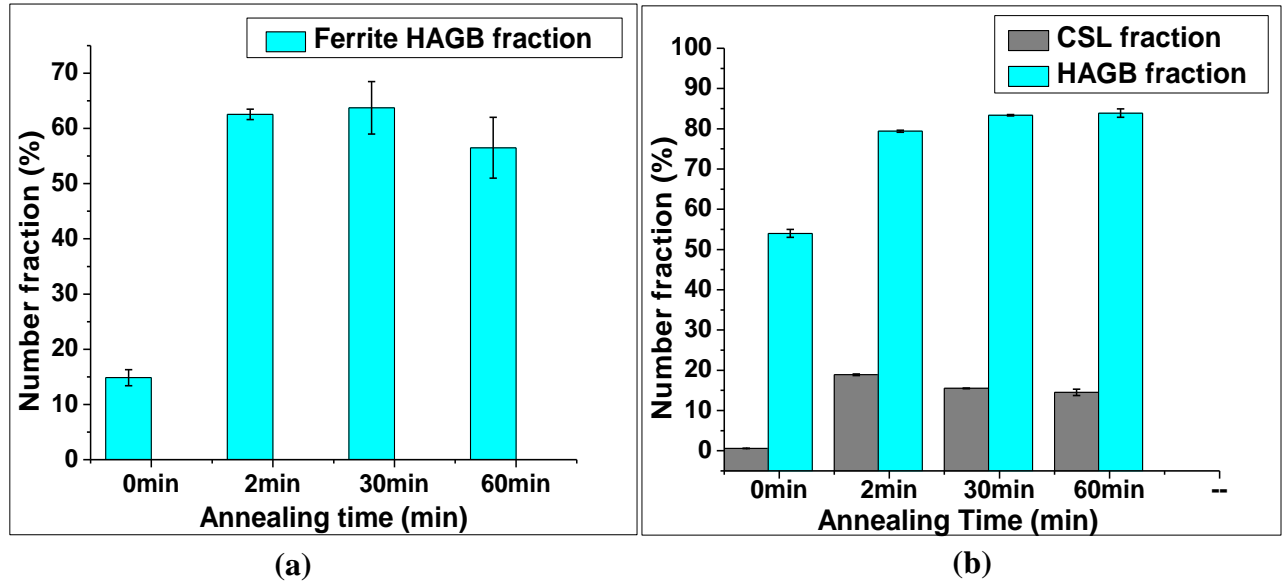
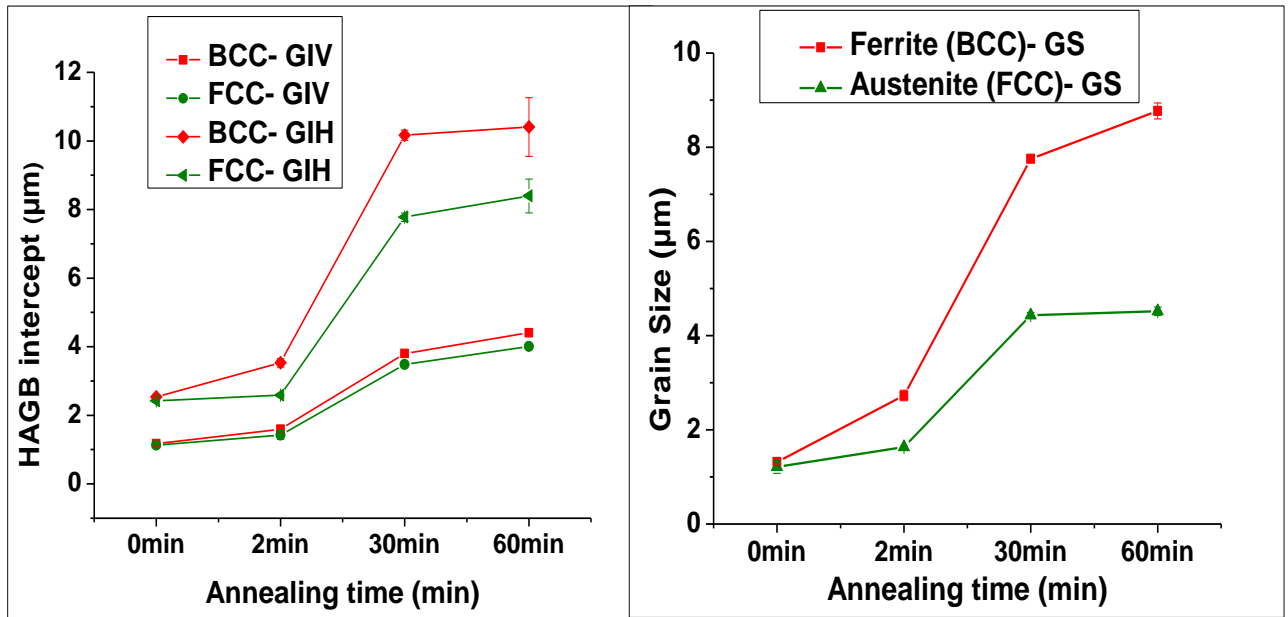


Fig. 4.11: (a) Ferrite- HAGB variation and (b) Austenite- HAGB & CSL variation with annealing time

Significant changes in key microstructural parameters, such as, HAGB intercept of phases along RD (horizontal grain intercept- GI_H) and ND (vertical grain intercept- GI_V) is observed during annealing. Careful observation of as warm rolled microstructure shows that each phase band contains many HAGBs and LAGBs due to grain fragmentation. In both phases, grain intercept along ND is increased with increasing isothermal holding time but significant change is not observed beyond annealing for 30 minutes (Fig. 4.12 (a)). Similar trend is observed for grain intercept along RD. However, grain intercept along RD (GI_H) is larger than that that along the ND (GI_V) in both the phases. Ferrite shows consistently higher grain size (the average grain size is obtained by fitting an ellipse) as compared to austenite (Fig. 4.12(b)).



(a) (b)
Fig. 4.12: (a) Variation of vertical and horizontal grain intercept and (b) Grain size variation with annealing time

4.5 Evolution of Texture during Annealing

Fig. 4.13 summarizes the evolution of texture during annealing. The evolution of texture in ferrite is shown by $\varphi_2=45^\circ$ section of the ODFs (Fig. 4.13((a)-(c))), while for austenite the (111) pole figures (Fig. 4.13((d)-(e))) are used. In order to clearly understand the texture evolution ideal locations of texture components in the ODF section for ferrite and pole figure for austenite are shown in Fig. 4.13(g) and 4.13(h), respectively.

Gradual changes can be seen in ODF section of ferrite during isothermal annealing (Fig. 4.13((a)-(c))). The RD-fiber is strengthened with increasing annealing time evident from the intensity distribution around the RD-fiber components. However, no significant change in intensity is observed for ND-fiber components. The evolution of texture is shown quantitatively in Fig. 4.14 which amply corroborates the ODF analysis.

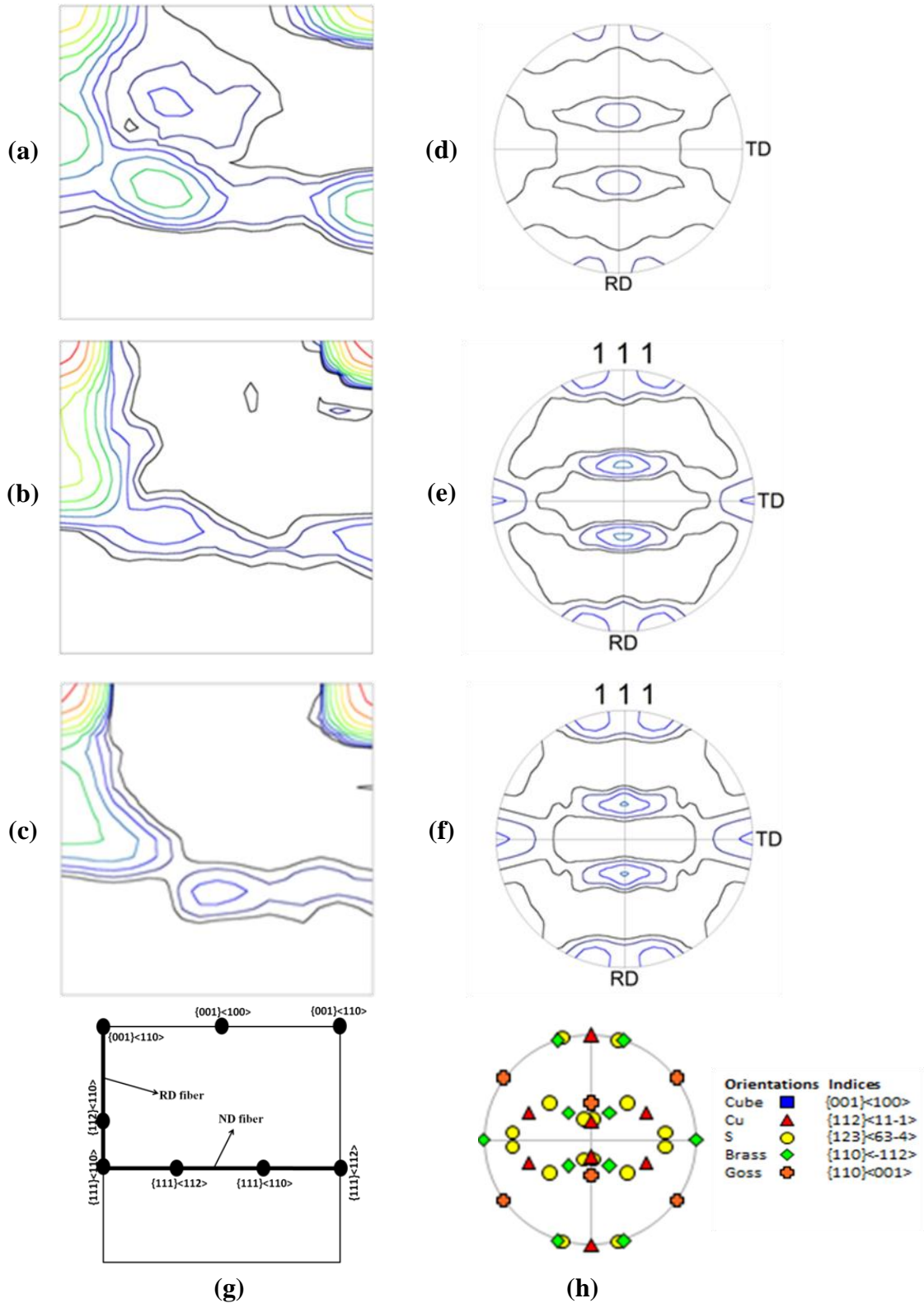


Fig. 4.13: (a)-(c) ϕ_2 45° section of ODF of ferrite and (d)-(f) (111) pole figure of austenite in annealed DSS, (g) ideal ODF of ferrite and (h) ideal (111) pole figure of austenite

The (111) pole figures of austenite in annealed DSS indicate the retention of pure metal type texture characterized by the presence of Cu, S and Bs components. No significant change in texture is observed even after isothermal holding for 60min (Fig. 4.13(d)-(e)). The brass recrystallization (BR) component ($\{236\}\langle 385\rangle$) which is often reported to be a strong component in the recrystallization texture of low SFE materials appears to be rather weak [12]. Similarly, Goss and twin of Goss (G^T : $\{111\}\langle 8\rangle\langle 4\ 4\ 11\rangle$) which are reported to be quite strong in cold-rolled and annealed DSS are rather weak in warm rolled and annealed DSS [12]. The evolution of texture in austenite is summarized quantitatively in Fig. 4.14 (b).

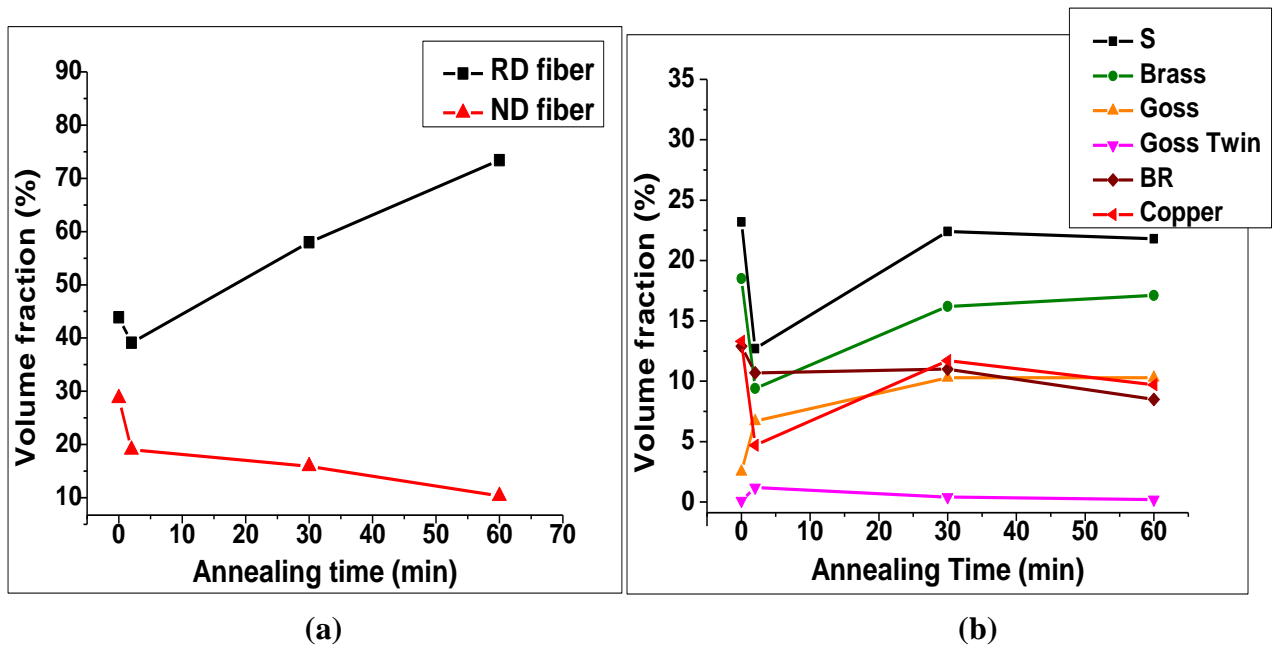


Fig. 4.14: Variation in RD and ND fiber in ferrite and (b) Variation in texture components in austenite of DSS with annealing time

4.5 Mechanical Properties of Duplex Stainless Steel

As mentioned in section 3.2 mechanical testing were carried out at room temperature using a strain rate of 10^{-3}sec^{-1} . Fig. 4.15 shows the engineering stress-strain plot of the as warm rolled DSS specimen (dimensions specified in section

3.2). Remarkable increase in the 0.2% offset yield strength to ~ 1.25 GPa and ultimate tensile strength to ~ 1.4 GPa is achieved with elongation to fracture $\sim 12\%$.

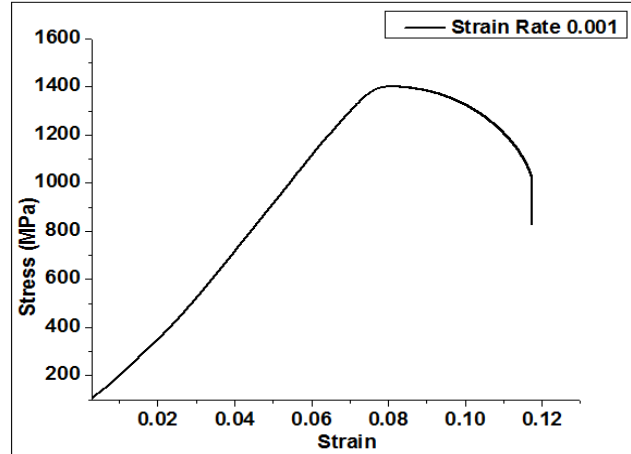


Fig. 4.15: Stress-strain plot of 90% warm-rolled DSS at 625°C.

Fig. 4.16 shows the schematic of the fractured specimen from where EBSD scan was acquired. Lamellar phase bands during tensile straining converge towards necking region. Intense shear is observed through the phase band near the necked region.

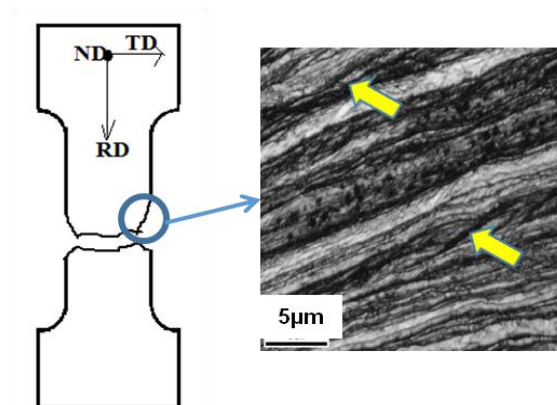


Fig. 4.16: Schematic of fractured specimen and IQ map at vicinity of necking region.

EBSD scans were taken close to fractured region on the ND-RD plane in a systematic manner. It is observed that as the necked region is approached the area fraction of austenite decreases systematically (Fig. 4.17). Nearly 40% austenite is

observed in the phase map of the as warm rolled DSS (Fig. 4.17(a)) which is further reduced to ~18% at 150 μ m away from the fractured (Fig. 4.17(b)) and is further reduced to ~3% at 5 μ m away from the fractured surface.

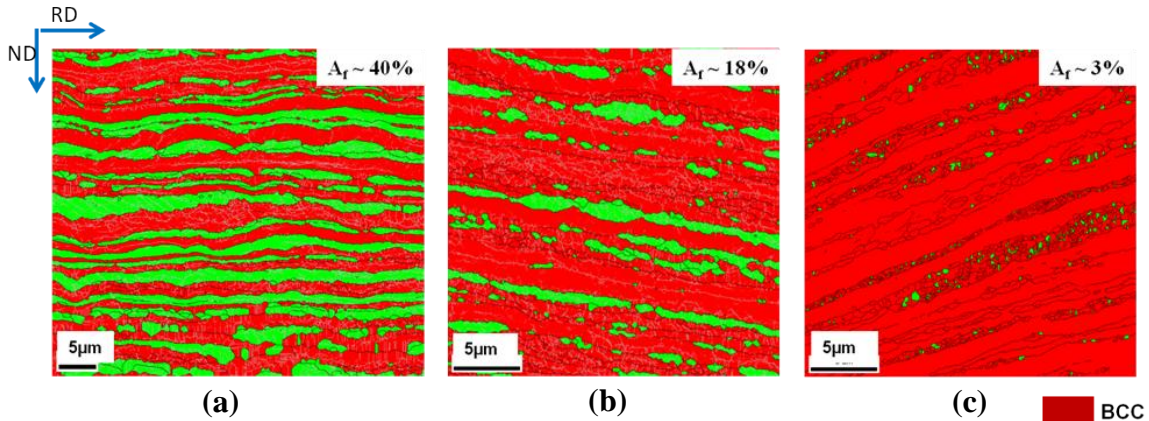


Fig. 4.17: Phase maps showing variation of austenite fraction at different regions (a) as warm rolled (b) 150 μ m and (c) 10 μ m away from the fractured surface in vicinity of necking region

Fig. 4.18 shows the engineering stress-strain plots of the as warm-rolled and isothermally annealed DSS for different time intervals. The tensile plots show improvement in ductility but the strength is significantly reduced. The yield strength; ultimate tensile strength and total elongation are summarized in Fig. 4.19.

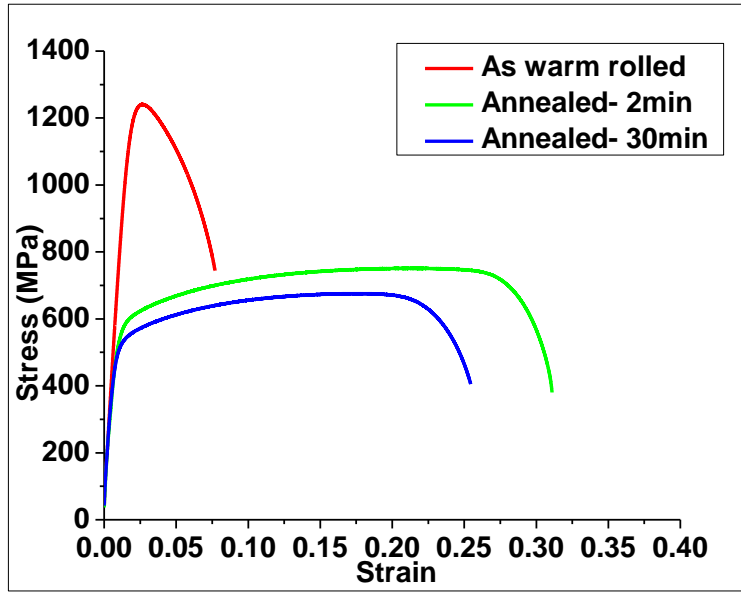


Fig. 4.18: Stress-strain plot of different thermo-mechanically treated DSS samples

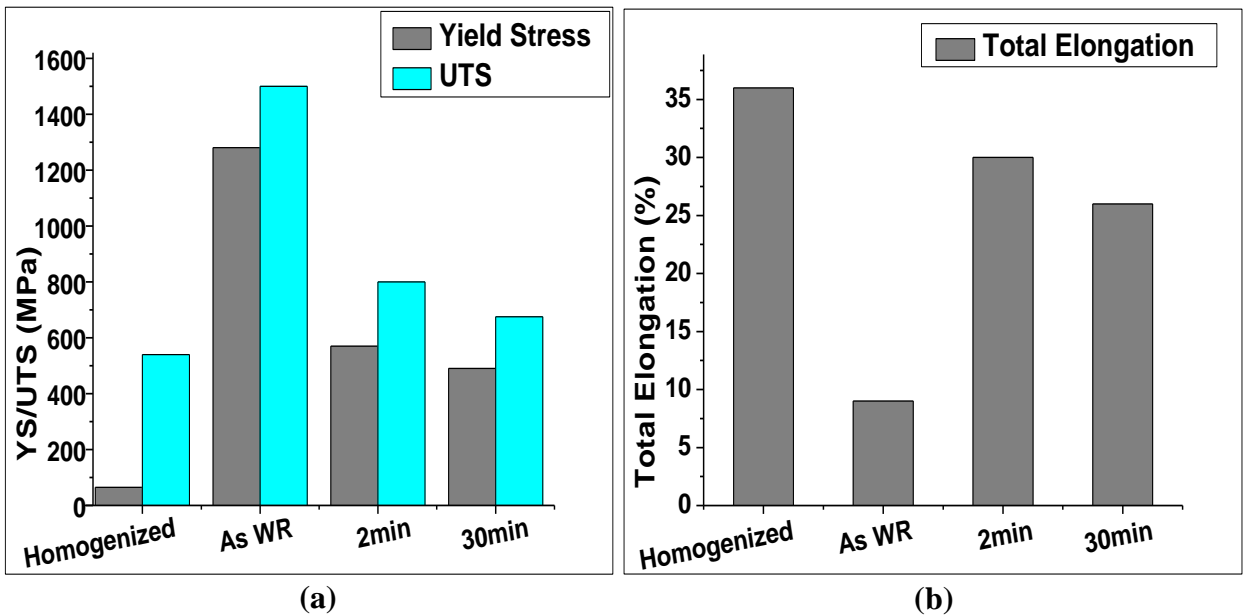


Fig. 4.19: (a) Yield strength and ultimate tensile strength and (b) total elongation of DSS in as warm-rolled and different isothermally annealed conditions.

Chapter 5: Discussion

In current study, evolution of microstructure and microtexture during warm rolling and isothermal annealing of commercial grade duplex steel is investigated. Subsequently the evolution of mechanical properties of different thermo-mechanically treated specimens is investigated separately.

5.1 Evolution of microstructure during warm rolling

There is no significant change observed in the area fraction of phases during warm rolling even up to heavy deformation level. This suggests that austenite is stable during warm-rolling so that microstructure and texture evolution during warm-rolling is not affected by phase transformation.

During warm-rolling the formation of typical lamellar deformation structure with alternate banded morphology elongated along the RD as observed in Fig. 4.4 is reported in duplex steels during cold-rolling and also during warm-rolling [12, 34]. The reduction in band-thickness in the two phases is similar at 90% warm rolled condition indicating that the two phases deform in a similar manner. Simultaneously there is significant internal subdivision is observed in individual phase as shown in Fig. 5.1. The formation of such fine lamellar structure could be attributed to the well-known grain sub-division mechanism. This internal phase band subdivision is supported by Fig. 4.5(a), where it is shown that decrease in grain size (GI) is more than that of phase band (PB).

5.2 Evolution of texture during warm rolling

Evolution of ferrite texture in DSS is characterized by two prominent texture fibers i.e. RD ($\langle 011 \rangle // \text{RD}$) fiber and ND ($\langle 111 \rangle // \text{ND}$) fiber. RD and ND fibers get

strengthened during cold working [27]. Barnett et al observed somewhat similar behavior during warm-rolling of single-phase ferritic steel [25].

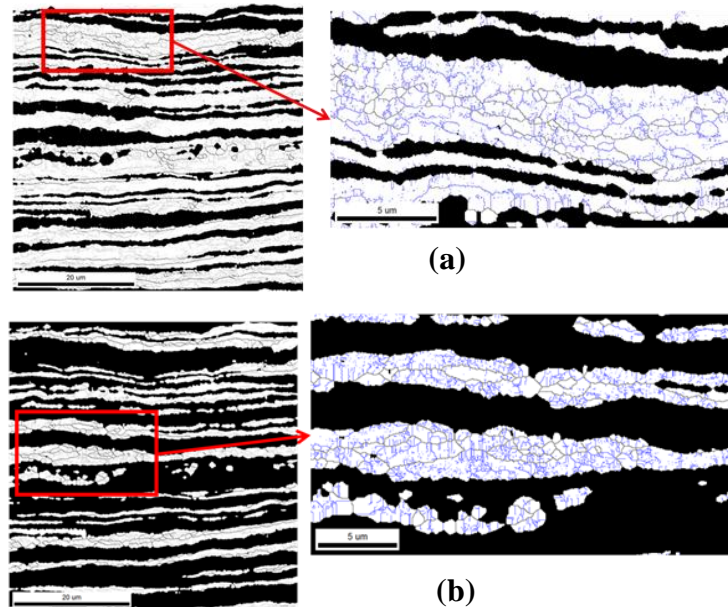


Fig. 5.1: GB maps of (a) ferrite and (b) austenite 90% warm rolled in DSS

Development of ferrite texture in DSS studied in this context shows strengthening of the RD fiber (volume fraction $\sim 45\%$) components which is evident from the $\phi_2 = 45^\circ$ section of the ODF (Fig. 4.6(e)-(h)). In contrast to the RD fiber, the ND fiber components in ferrite of warm rolled DSS are weak. Quantitatively, this is evident from Fig. 4.7 that RD fiber dominates over ND fiber with increasing reduction. Thus, it is justified that microstructure and microtexture of two phases in DSS is greatly affected by warm rolling temperature which also agrees with the experimental observations of Bhattacharjee et. al.

As it is clearly visible, in Fig. 4.8(e)-(h), that during warm rolling, austenite in DSS develops pure metal type deformation texture with strong Cu, S and Bs components. This behavior is in stark contrast with that observed during cold rolling

of DSS and single phase austenitic steel where strong brass type texture is observed in austenite after heavy cold rolling [12]. Deformation twins evolved in microstructure of low SFE materials are responsible for texture transition from metal type to brass type texture [30]. This can be explained based on the facts that the stacking fault energy (SFE) is increased during warm-rolling so that the formation of deformation twins is suppressed in favor of usual dislocation slip. Recent results published by Bhattacharjee et al. also support this behavior.

5.3 Evolution of microstructure during annealing

During annealing of 90% warm rolled DSS evolution of globular morphology from lamellar structure is observed (Fig. 4.10). The annealing was carried out at the same temperature of homogenization treatment to minimize the phase transformation during annealing. This is clearly observed from Fig. 4.16 where austenite fraction of ~40% is maintained in the DSS. However, immediately after annealing for 2mins the area fraction of austenite is observed to be increase. This could be due to the fact that since the annealing is carried out in a conventional furnace the annealing time of 2mins is not sufficient to establish the equilibrium in the phase fraction. Since for such short annealing time larger part of the time the sample remains at lower temperature than the isothermal annealing temperature conversion of austenite to ferrite is quite possible. The phase equilibrium is reached as expected for longer isothermal holding time.

Careful observation of phase maps of both annealed DSS (Fig. 4.10) shows that there is gradual transition from lamellar to bamboo type morphology finally to globular morphology throughout microstructures, which is schematically represented in Fig. 5.3.

The origin of the bamboo type morphology may be explained recovery behavior of ferrite [34]. Since the deformation is carried out at the warm-rolling temperature ferrite is already recovered at that temperature. As a result the internal misorientation build-up inside the ferrite bands is quite low. Therefore, during annealing the subgrains inside the ferrite bands will be constrained to grow along the RD (due to the presence of austenite bands as immediate

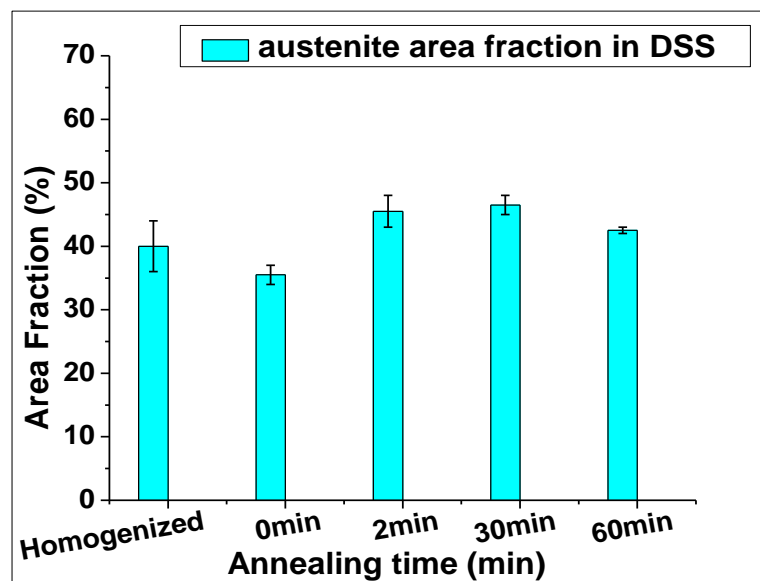


Fig. 5.2: Variation of area fraction of austenite in DSS during isothermal annealing

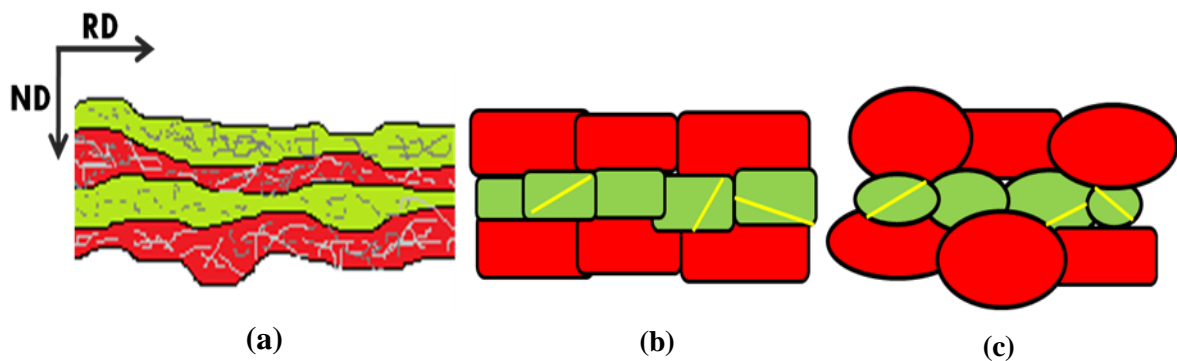


Fig. 5.3: (a) As warm rolled (90%) alternate lamellar structure (b) Short time annealing (c) Longer time annealing globular morphology

along the ND) and impinge with neighboring subgrains separated with them by low angle boundaries. This will evidently result in the bamboo type morphology observed for the ferrite bands.

In contrast the austenite shows discontinuous recrystallization during isothermal annealing. This is quite evident from large fraction of HAGBs in austenite and presence of profuse annealing twin boundaries (Fig. 4.12). Discontinuous recrystallization in austenite as opposed to predominantly recover in ferrite also leads to higher aspect ratio in austenite as compared to ferrite.

5.4 Evolution of annealing texture

The characteristic softening behavior of the two phases explained in following context. As already stated the ferrite undergoes pronounced recovery. Since recovery proceeds without nucleation of strain free grains as in the case of discontinuous recrystallization the characteristics of the deformation texture will be retained. In ferrite the RD fiber components, such as, $\{001\}\langle 110\rangle$ and $\{112\}\langle 110\rangle$ would preferentially undergo recovery while the ND-fiber components $\{111\}\langle 110\rangle$ and $\{111\}\langle 112\rangle$ due to their higher stored energy and frequency advantage tend to show a recrystallization type behavior during annealing[13, 35]. So, ferrite in DSS after different isothermal annealing treatments shows remarkably higher amount of RD fiber components (Fig. 4.14(a)) as compared to the ND fiber components due to pronounced recovery which amply corroborates the microstructural development. The recovery of ferrite is also further aided by dynamic recovery during warm-rolling which reduces the driving force for recrystallization greatly.

The austenite in different isothermally annealed DSS retains pure metal type texture (Fig. 4.8(e)-(h)) of austenite in as warm-rolled material. This indicates

recrystallization without any preferential orientation selection so that the recrystallization texture is a random sampling of deformation texture. It may be seen in Fig. 4.14(b) that BR component $\{236\}\langle 385\rangle$ which is often reported as a strong recrystallization texture component in low SFE material showing to the nucleation of this component in shear bands and subsequent growth selection of these grains due to the $40^\circ\langle 111\rangle$ relationship with the B_S is rather weak [11]. This is probably due to the fact that the brass component is quite low in the deformation texture of warm-rolled DSS. However, the G and G^T components are remarkably absent unlike cold rolled and annealed DSS. Since the fraction of G component is low in deformation texture, upon annealing the fraction of both G and G^T remains low unlike the cold-rolled and annealed DSS.

Thus, the two phases show recrystallization behavior independent of each other and the texture evolution is determined by their characteristic recrystallization behavior. However, the grain growth of two phases in DSS is strongly affected by the presence of the other phase.

5.5 Mechanical Properties of DSS

The remarkable increase in strength during warm rolling (Fig. 4.15) is attributed to the formation of ultrafine microstructure and phase bands which act as additional barrier to dislocation motion. As, tensile test is carried out along RD all phase bands are aligned parallel to the tensile axis. One crucial observation is that at the vicinity of the necked region there is gradual decrease in austenite content. Austenite fraction of 40% in the as warm rolled DSS is reduced drastically to ~18% at the region 150 μm away from fractured surface and is further reduced to just 3% at 10 μm away from fracture as shown in Fig. 4.17. This possibly indicates that

austenite is transformed to martensite (which is indexed as a bcc phase during EBSD measurements) locally due to stress concentration in the necked region. Indirect evidence of this is obtained from the IQ map obtained at the vicinity of the necked region which shows great variation in the IQ distribution in the ferrite phase (Fig. 4.16).

Tensile testing carried out for different isothermally treated samples shows that with increase in annealing time strength of DSS decrease. At same time ductility significantly increased from 11% for warm rolled sample to 30% for 30min annealed sample. Thus, thermo-mechanical processing combining warm rolling and isothermal annealing can yield very attractive mechanical properties and should be investigated in future research.

Chapter 5: Summary and Conclusions

The evolution of microstructure and microtexture during warm-rolling and subsequent recrystallization has been investigated in a commercial grade SAF 2507 duplex steel. The DSS has been rolled 625°C and isothermally annealed at 1150°C for different time intervals. The following major conclusions may be drawn from the present study:

1. Ultrafine lamellar structure with alternate arrangement of two phases can be produced during warm rolling.
2. Ferrite texture in warm rolled DSS is characterized by stronger RD fiber as compared to the ND-fiber.
3. Austenite texture in warm rolled DSS yields pure metal type texture even after heavy deformation. This is attributed to the suppression of deformation twins in favor of dislocation slip at the warm-rolling temperature.
4. Annealing of the DSS is characterized by gradual transformation from lamellar bamboo type morphology to a more globular morphology with increasing isothermal annealing time. The microstructural break-down during annealing is explained by the mechanism of mutual interpenetration of the two phases along the grain boundaries at the triple points.
5. Very limited grain growth of the two phases observed even after annealing for long duration is attributed to the growth inhibition due to the presence of the other phase.

6. Ferrite in DSS after different isothermal annealing treatment gives remarkably higher amount of RD-fiber components than that of ND-fiber components due to pronounced recovery.
7. Austenite in annealed DSS, however, retains pure metal type texture, this indicated recrystallization without preferential orientation selection.
8. The texture evolution of the two phases could be explained by the behavior of the respective single phase materials. Therefore, the texture development of the two phases is not significantly affected by the presence of the other phase while the grain growth during recrystallization is strongly affected by the presence of the other phase.
9. Ultra high strength obtained of warm rolled DSS possibly originates from formation of ultrafine microstructure and possible role of finely spaced phase boundaries as additional barrier to dislocation motion.
10. The present results demonstrate that warm rolling can be used successfully for developing ultrahigh strength DSS.

References

- [1] Godfrey, A., D.J. Jensen, and N. Hansen, Slip pattern, microstructure and local crystallography in an aluminium single crystal of copper orientation $\{112\}\langle 111\rangle$. *Acta Materialia*, 1998. 46(3): p. 835-848.
- [2] Bay, B., et al., Overview No-96 - Evolution of Fcc Deformation Structures in Polyslip. *Acta Metallurgica Et Materialia*, 1992. 40(2): p. 205-219.
- [3] R. E. Bauer. Rudolf, Heinrich Mecking, and Kurt Lücke, Textures of copper single crystals after rolling at room temperature, *Materials Science and Engineering* 27.2, (1977) 163-180.
- [4] J. Hirsch, K. Lücke, and M. Hatherly, Overview No. 76, Mechanism of deformation and development of rolling textures in polycrystalline f.c.c. Metals-III. The influence of slip inhomogeneities and twinning, *Acta Metallurgica*, 36.11, (1988) 2905-2927.
- [5] J. Hirsch and K. Lücke, Overview no. 76. Mechanism of deformation and development of rolling textures in polycrystalline f.c.c. metals-I. Description of rolling texture development in homogeneous CuZn alloys, *Acta Metallurgica*, 36.11, (1988) 2863-2882.
- [6] R. K. Ray, Rolling textures of pure nickel, nickel-iron and nickel-cobalt alloys. *Acta Metallurgica EtMaterialia*, 43.10, (1995) 3861-3872.
- [7] T. Leffers and R. K. Ray, The brass-type texture and its deviation from the copper-type texture, *Progress in Materials Science* 54.3, (2009) 351-396.
- [8] L.S. Toth, J.J. Jonas, R.K. Ray, Development of ferrite rolling texture in low and extra low carbon steels, *Metallurgical Transactions, A*, 21A, (1990) 1990-2985.
- [9] F.J. Humphreys, M. Hatherly, *Recrystallization and Related Annealing Phenomenon*, 2nd ed., Elsevier, Oxford, 2004.

- [10] S.K. Ghosh, D. Mahata, R. Roychaudhari, R. Mondal, 2012, Effect of rolling deformation and solution treatment on microstructure and mechanical properties of a cast duplex stainless steel *Bull. Materials Science*, vol. 35, pp. 839-846.
- [11] J. Keichel, J. Foct, and G. Gottstein: *ISIJ Int.*, 2003, vol. 43, pp. 1788–94.
- [12] J. Keichel, J. Foct, and G. Gottstein: *ISIJ Int.*, 2003, vol. 43, pp. 1781–87.
- [13] J. Keichel, G. Gottstein, and J. Foct: *High Nitrogen Steels '98, 1999*, vol. 318–23, pp. 785–91.
- [14] A. Belyakov, Y. Kimura, and K. Tsuzaki: *Acta Materialia*, 2006, vol. 54, pp. 2521–32.
- [15] M. Blicharski, J. Jura, T. Baudin, R. Penelle, J. Bonarski, and M. Kowalski: *Arch. Metall. Mater.*, 2005, vol. 50, pp. 495–502.
- [16] K.E. Cooke, S. Yang, C. Selcuk, A. Kennedy, D.G. Teer, and D. Beale: *Surf. Coat. Technol.*, 2004, vol. 188, pp. 697–702.
- [17] J. Rys and W. Ratuszek, *Appl. Cryst.* XXI, 2010, vol. 163, pp. 145–50.
- [18] J. Rys and A. Zielinska-Lipiec, *Arch. Metall. Mater.*, 2012, vol. 57, pp. 1041–53.
- [19] J. Rys and M. Witkowska: *Appl. Cryst.* XXI, 2010, vol. 163, pp. 151–56.
- [20] J. Hamada and N. Ono: *Mater. Trans.*, 2010, vol. 51, pp. 635–43.
- [21] J. Rys, W. Ratuszek, and M. Witkowska, *Arch. Metall. Mater.*, 2005, vol. 50, pp. 857–70.
- [22] J. Rys, W. Ratuszek, and M. Witkowska, *Appl. Cryst.* XX, 2007, vol. 130, pp. 57–62.
- [23] M.R. Toroghinejad, A.O. Humphreys, F. Ashrafizadeh, A. Najafizadeh, and J.J. Jonas: *Mater. Sci. Forum*, 2003, vols. 426–4, pp. 3691–96.

- [24] R.K. Ray and A. Haldar: *Mater. Manuf. Process.*, 2002, vol. 17, pp. 715–29.
- [25] M.R. Barnett and J.J. Jonas: *ISIJ Int.*, 1999, vol. 39, pp. 856–73.
- [26] A. Belyakov, R. Kaibyshev, Y. Kimura, and K. Tsuzaki: *Mater.Sci. Forum*, 2010, vols. 638–642, pp. 1905–10.
- [27] R.K. Ray: *Acta Metall. Mater.*, 1995, vol. 43, pp. 3861–72.
- [28] R.E. Smallman and D. Green: *Acta Metall.*, 1964, vol. 12, pp. 145–54.
- [29] R. Saha and R.K. Ray, *J. Mater. Sci.*, 2007, vol. 42, pp. 9548–52.
- [30] T. Leffers and R.K. Ray, *Prog. Mater. Sci.*, 2009, vol. 54, pp. 351–96.
- [31] G. Wassermann and J. Grewen, *Texturen Metallischer Werkstoffe*, Springer, Berlin, 1962.
- [32] P.C.J. Gallagher: *Metall. Trans.*, 1970, vol. 1, pp. 2429–61.
- [33] R.M. Latanision and A.W. Ruff: *Metall Trans.*, 1971, vol. 2, pp. 505–09.
- [34] P.P. Bhattacharjee, M. Zaid, Dan G., B. Bhadak, *Met. Trans. A*, 45A, pp. 2180-2119.
- [35] J. Hamada and N. Ono: *Mater. Trans.*, 2010, vol. 51, pp. 635–43.